

Entropy mapping of the outer electron radiation belt between the magnetotail and geosynchronous orbit

Joseph E. Borovsky^{1,2} and Thomas E. Cayton¹

Received 12 January 2011; revised 22 March 2011; accepted 1 April 2011; published 28 June 2011.

[1] The specific entropy (entropy density) S is examined for the outer electron radiation belt at geosynchronous orbit and for the energetic electron population in the Earth's magnetotail. The outer electron radiation belt is measured with the SOPA detectors on board six geosynchronous satellites and the energetic electrons of the magnetotail are measured with instrumentation on board 12 Global Positioning Satellites (GPS) with a magnetic field model used to map the GPS orbit to the magnetotail. Density n and temperature T values are determined from relativistic Maxwellian fits to the electron measurements, enabling the specific entropy S to be calculated. For low temperatures the nonrelativistic specific entropy is $S = T/n^{2/3}$; for a relativistic Maxwellian distribution a relativistically correct expression for $S = S(T,n)$ is derived and used. The outer electron radiation belt at geosynchronous orbit local midnight ($n \sim 3 \times 10^{-4} \text{ cm}^{-3}$ and $T \sim 140 \text{ keV}$) and the energetic-electron population in the magnetotail ($n \sim 1 \times 10^{-4} \text{ cm}^{-3}$ and $T \sim 50 \text{ keV}$) statistically have the same specific entropy. Hence the two populations are probably the same. This implies adiabatic transport (1) from the magnetotail to the dipole (where the magnetotail electrons are the source of the outer electron radiation belt) or (2) from the dipole to the magnetotail (where the magnetotail electrons are leakage from the radiation belt).

Citation: Borovsky, J. E., and T. E. Cayton (2011), Entropy mapping of the outer electron radiation belt between the magnetotail and geosynchronous orbit, *J. Geophys. Res.*, 116, A06216, doi:10.1029/2011JA016470.

1. Introduction

[2] The origin of the Earth's electron radiation belt is an outstanding issue in magnetospheric physics; another outstanding issue is the transport of energetic electrons between the inner magnetosphere, the outer magnetosphere, the cusp, and the magnetotail. Several sources (seed populations) for the outer electron radiation belt have been suggested, including energetic particles in the solar wind [Li *et al.*, 1997], substorm electron injections [Ingraham *et al.*, 2001; Fok *et al.*, 2001], suprathermal electrons in the plasma sheet [McDiarmid and Burrows, 1965; Borovsky *et al.*, 1998a; Obara *et al.*, 2001; Varotsou *et al.*, 2005], the cusp [Fritz and Chen, 1999; Fritz *et al.*, 2000], and the outer magnetosphere [Bezrodnykh *et al.*, 1984a, 1984b, 1987]. This report commences the use of specific entropy measurements to connect particle populations to the electron radiation belt. The population focused on is the energetic electron population in the magnetotail (M. H. Denton and T. E. Cayton, Density and temperature of energetic electrons in the Earth's magnetotail derived from high-latitude GPS observations during the declining phase of the solar cycle, submitted to *Geophysical Research Letters*,

2011), a population more energetic than the suprathermal tail of the electron plasma sheet.

[3] Examining the value of the specific entropy $S = T/n^{2/3}$ in time series data is a powerful method of identifying plasmas. For several applications in space physics the specific entropy has been used to identify and differentiate plasmas in the solar wind [Burlaga *et al.*, 1990; Crooker *et al.*, 1996; Burton *et al.*, 1999; Osherovich *et al.*, 1999; Lazarus *et al.*, 2003; Neugebauer *et al.*, 2004; Pagel *et al.*, 2004; Borovsky, 2008a] and in the magnetosphere [Goertz *et al.*, 1991; Wing *et al.*, 2007]. Typical specific entropy values for several ion and electron populations in the solar wind and magnetosphere are collected in Table 1, including the values for the outer electron radiation belt calculated in this report. The various specific entropy values from Table 1 are plotted in Figure 1, where it is seen that the specific entropy of the outer electron radiation belt is orders of magnitude higher than the specific entropy of the other collected populations.

[4] The concept that the specific entropy $S = T/n^{2/3}$ of a plasma can be conserved under special conditions has been used to explore plasma transport issues in the plasma sheet of the Earth's magnetotail [e.g., Schindler, 1975; Erickson and Wolf, 1980; Schindler and Birn, 1982; Birn and Schindler, 1983; Huang *et al.*, 1989; Baumjohann and Paschmann, 1989; Spence and Kivelson, 1990; Zhu, 1990; Goertz and Baumjohann, 1991; Borovsky *et al.*, 1998b; Birn *et al.*, 2009; Johnson and Wing, 2009] and evolution issues for the solar wind [e.g., Eyni and Steinitz, 1978; Schwartz

¹Los Alamos National Laboratory, Los Alamos, New Mexico, USA.

²Department of Atmospheric Oceanic and Space Science, University of Michigan, Ann Arbor, Michigan, USA.

Table 1. Typical Values of the Specific Entropy $S = T/n^{2/3}$ for Several Ion and Electron Populations in the Solar Wind and Earth's Magnetosphere^a

Particle Population	n, cm^{-3}	T, eV	$S, \text{eV cm}^2$	Reference
Inner plasmasphere ions and electrons	2000	0.5	3×10^{-3}	Comfort [1986]
Outer plasmasphere ions	100	0.75	3.5×10^{-2}	Sojka and Wrenn [1985]
Slow solar wind ions 0.3 AU	90	14	0.7	Helios 0.29 – 0.35 AU
Fast solar wind ions 0.3 AU	30	44	4.5	Helios 0.29 – 0.35 AU
Slow solar wind electrons 0.3 AU	90	25	1.2	Marsch <i>et al.</i> [1989]
Fast solar wind electrons 0.3 AU	30	20	2.0	Marsch <i>et al.</i> [1989]
Slow solar wind ions 1 AU	5	5	1.7	Borovsky and Denton [2010b]
Fast solar wind ions 1 AU	3	20	10	Borovsky and Denton [2010b]
Slow solar wind electrons 1 AU	5	20	7	Skoug <i>et al.</i> [2000]
Fast solar wind electrons 1 AU	3	20	10	Skoug <i>et al.</i> [2000]
Magnetosheath ions nose: slow wind	20	500	70	Borovsky [2008b]
Magnetosheath ions nose: fast wind	12	1700	325	Borovsky [2008b]
Magnetosheath ions flank: slow wind	8	10	2.5	Paularena <i>et al.</i> [2001]
Magnetosheath ions flank: fast wind	5	50	15	Paularena <i>et al.</i> [2001]
LLBL ions dayside	5	500	170	Phan and Paschmann [1996]
LLBL ions flanks	5	500	170	ISEE-2 magnetotail
Magnetotail CDPS	1.5	500	750	Fujimoto <i>et al.</i> [2000]
Geosynchronous CDPS	5	2000	700	Thomsen <i>et al.</i> [2003]
Near-Earth magnetotail EPS	0.23	900	2500	Baumjohann [1993]
Geosynchronous EPS	0.8	2000	2300	Denton <i>et al.</i> [2005]
Distant tail IPS	0.074	2400	1.4×10^4	Borovsky <i>et al.</i> [1998b]
Near-Earth tail IPS	0.23	5800	1.6×10^4	Borovsky <i>et al.</i> [1998b]
Geosynchronous IPS	0.84	8500	9.6×10^3	Borovsky <i>et al.</i> [1998b]
Distant-tail energetic electrons	7.7×10^{-5}	41,000	2.7×10^7	this report
Near-Earth-tail energetic electrons	1.2×10^{-4}	52,000	2.6×10^7	this report
OERB geosynchronous	3.4×10^{-4}	140,000	5.0×10^7	this report

^aThe following notation is used: LLBL, low-latitude boundary layer; CDPS, cold dense plasma sheet; EPS, electron plasma sheet; IPS, ion plasma sheet; OERB, outer electron radiation belt. Note for the final three rows, the relativistic expression for the specific entropy (expression (5)) is used.

and Marsch, 1983; Freeman and Lopez, 1985; Freeman, 1988; Marsch *et al.*, 1989; Whang *et al.*, 1989; Goldstein *et al.*, 1995], magnetic clouds [e.g., Osherovich *et al.*, 1997; Gosling, 1999; Farrugia *et al.*, 1999], and the Earth's plasma sheet [Goertz *et al.*, 1991; Huang *et al.*, 1989, 1992; Wing *et al.*, 2007; Wing and Johnson, 2009]. Further, in a collisionless plasma, S can be conserved separately for the ions and the electrons, preserving such quantities as the ion-to-electron temperature ratio of the plasma [cf. Lavraud and Borovsky, 2008; Lavraud *et al.*, 2009].

[5] The specific entropy $S = T/n^{2/3}$ as a conserved quantity is a concept for an adiabatic gas which collisionally remains isotropic [cf. Jeans, 1954]. The isotropy assumption is built into the selection of the adiabatic index Γ being $\Gamma = 5/3$, which gives the 2/3 exponent in the expression for S. For some of the plasmas of interest in space physics, isotropization might be a slow process; for example, for the solar wind at 1 AU the electron isotropization time and ion isotropization time owing to Coulomb scattering are 8×10^3 s = 2.3 h and 1×10^5 s = 33 h, respectively [Borovsky and Gary, 2011], and for the magnetotail plasma sheet the ion isotropization time owing to Coulomb scattering is 1×10^9 s = 3000 years [Borovsky *et al.*, 1997], although electromagnetic plasma waves may speed up the isotropization. For the outer electron radiation belt at geosynchronous orbit with a temperature of ~ 150 keV, the whistler chorus pitch angle diffusion coefficient is $D_{\alpha\alpha} \sim 10^{-4} \text{ s}^{-1}$ [cf. Horne *et al.*, 2006; R. Horne, private communication, 2010], which gives an isotropization time of $\sim 10^4$ s ~ 3 h. Even though isotropy is not fully enforced in plasma populations, the use of S to track plasma transport has been successful [e.g., Borovsky *et al.*, 1998b; Marino *et al.*, 2008; Smith *et al.*, 2001; Breech *et al.*, 2009; Stawarz *et al.*, 2009; Isenberg *et al.*, 2010].

Recently, the anisotropy of the outer electron radiation belt at geosynchronous orbit was surveyed [Borovsky and Denton, 2011], whereas electrons with energies greater than 1 MeV can exhibit high anisotropies (with parallel-to-B fluxes dominating over perpendicular-to-B fluxes at local midnight [cf. Kaye *et al.*, 1978; Selesnick and Blake, 2002; Fritz *et al.*, 2003]), for the bulk of the outer electron radiation belt with energies of 100–200 keV the electrons are quasi-isotropic at geosynchronous orbit [cf. Borovsky and Denton, 2011, Figures 2 and 6]. The energetic electrons in the magnetotail are reported to be approximately isotropic [e.g., Hones *et al.*, 1968; Retzler and Simpson, 1969; Sarris *et al.*, 1976].

[6] In the work of Borovsky and Denton [2009] and Borovsky and Denton [2010a] the specific entropy of the outer electron radiation belt at geosynchronous orbit was briefly examined with a focus on the changes in the specific entropy associated with prestorm electron precipitation and with storm-time electron heating. In this report the specific entropy of the outer electron radiation belt at geosynchronous orbit will be further examined, as will the specific entropy of the energetic electron population of the magnetotail.

[7] This report is organized as follows. In section 2.1 a single-particle definition of the specific entropy S is derived and in section 2.2 a relativistic expression for the specific entropy S is derived for relativistic Maxwellian populations. In section 3 the relativistic specific entropy of the outer electron radiation belt at geosynchronous orbit is examined and in section 4 the relativistic specific entropy of the energetic electrons in the magnetotail is examined. In section 5 the outer electron radiation belt at geosynchronous orbit and the energetic electron population in the magnetotail are

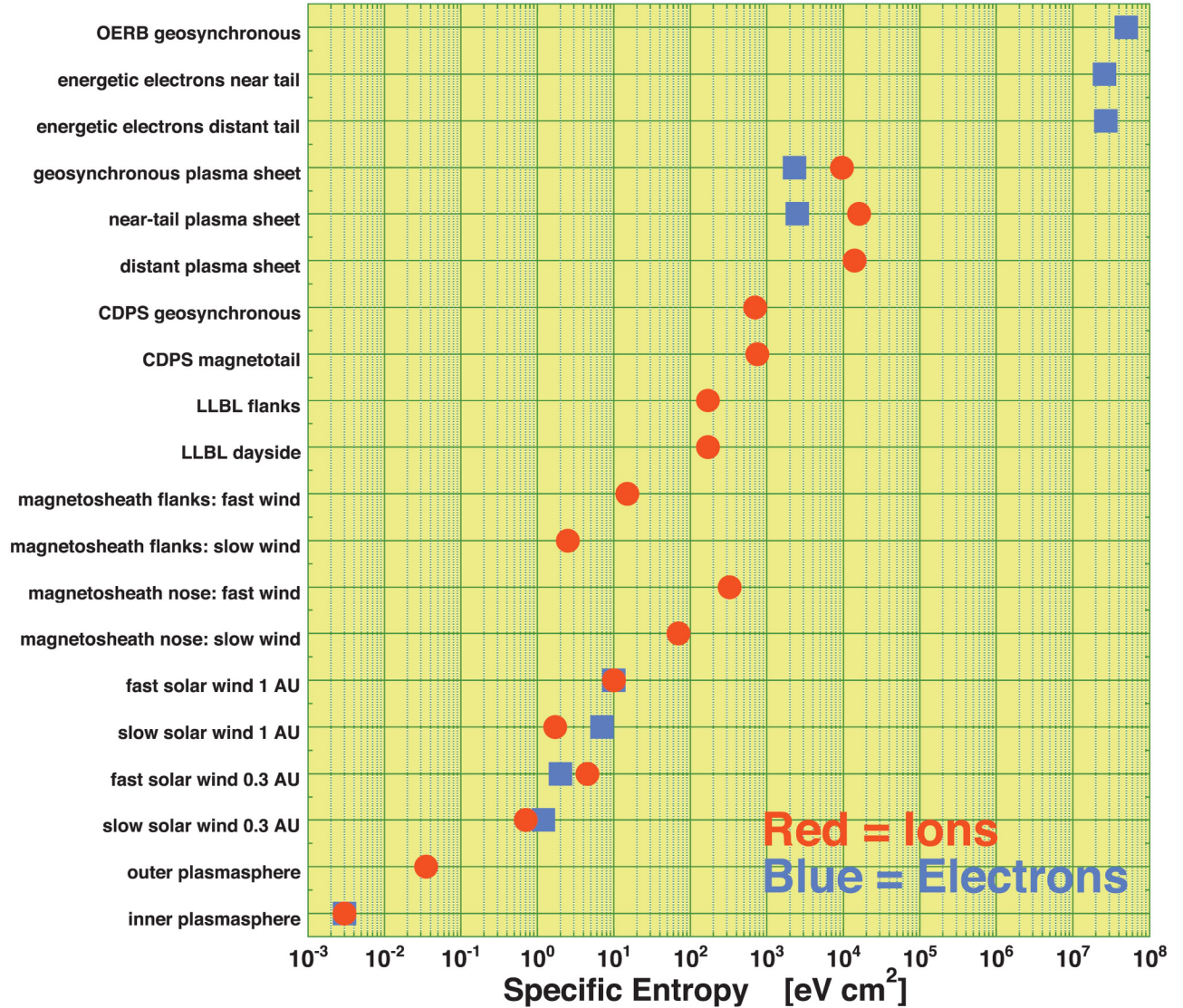


Figure 1. Typical specific entropy values $S = T/n^{2/3}$ are plotted for several ion and electron populations in the solar wind and magnetosphere. Details can be found in Table 1.

successfully matched up. Section 6 contains discussions about adiabatic transport of energetic electrons in the outer magnetosphere and magnetotail. The report is summarized in section 7.

2. Specific Entropy for Energetic Particle Populations

[8] Pertinent to the energetic electrons in the Earth's magnetosphere, in this section a single-particle interpretation of the specific entropy is given (section 2.1) and a relativistic expression for the specific entropy is derived (section 2.2).

2.1. Specific Entropy and the Adiabatic Invariants per Unit Flux

[9] For a gas the specific entropy S is conserved as the fluid advects: this is written $dS/dt = 0$ [cf. Schindler and Birn, 1978; Goertz and Baumjohann, 1991]. For a gas with a Polytropic index Γ (= ratio of specific heats), the specific

entropy (entropy per unit mass) is $P^{1/\Gamma}/n$ [cf. Birn *et al.*, 2009], but in principle it can be redefined in the more familiar form $Pn^{-\Gamma}$, where P is the particle pressure of the gas and n is the number density of gas particles. With $P = nk_B T$, the redefined specific entropy is $S = T/n^{\Gamma-1}$. For an adiabatic gas in three dimensions $\Gamma = 5/3$ and the specific entropy S is

$$S = T/n^{2/3} \quad (1)$$

Note that the entropy itself can be expressed as $C_v \log(S)$ [cf. Boyd and Sanderson, 1969, equation (6–20)], where C_v is the specific heat at constant volume.

[10] The specific entropy $S = T/n^{2/3}$ as a conserved quantity is a concept for an adiabatic gas or adiabatic plasma which collisionally remains isotropic [cf. Bernstein *et al.*, 1958; Kulsrud, 1983] (but see Montgomery [1971, equation (2–5)]). The isotropy assumption is built into the selection of the adiabatic index Γ being $\Gamma = 5/3$. In this section it is shown that the specific entropy $S = T/n^{2/3}$ of a collisionless plasma

can also be expressed in terms of the first two adiabatic invariants of the particles plus two other conserved quantities. When a population of charged particles in a dipole magnetic field is constantly isotropized (e.g., by pitch angle scattering), then the behavior of the population is adiabatic (as shown in Appendix 2 of Borovsky *et al.* [1981]); if the isotropization is not constantly enforced, the population undergoes nonadiabatic evolution [cf. Goertz, 1978].

[11] The first adiabatic invariant is $\mu = p_{\perp}^2/B$ [e.g., Alfvén and Falthammar, 1963; Borovsky and Hansen, 1991] where $p_{\perp} = mv_{\perp}$ is the component of the momentum of a particle perpendicular to the magnetic field B . For an isotropic population of particles with temperature T , a thermal particle has a velocity given by $v_{\perp}^2 = k_B T/m$ and the first adiabatic invariant can be redefined (nonrelativistically) as $\mu = T/B$. The second adiabatic invariant is $J = 2 \int p_{\parallel} ds$ [e.g., Northrop and Teller, 1960; Alfvén and Falthammar, 1963], where $p_{\parallel} = mv_{\parallel}$ is the component of the momentum of a particle parallel to the magnetic field B and the integral $\int ds$ is over the length of a flux tube. The integral $\int p_{\parallel} ds$ can be approximated as $p_{\parallel} L$ where L is the length of a flux tube. Assuming isotropy, $v_{\parallel} = (k_B T/m)^{1/2}$ for a thermal particle and the second adiabatic invariant can be rewritten $J = T^{1/2}L$. The third conserved quantity for a population of particles in the magnetosphere is the number of particles N in a flux tube. This number can be written as $N = nV$, where n is the number density of particles and V is the spatial volume of the flux tube. Writing the volume of the flux tube as $V = AL$, where A is the cross-sectional area of the flux tube and L is the length of the flux tube, the number of particles is expressed as $N = nAL$. The final conserved quantity is the total magnetic flux B in the flux tube, which can be written as $B = BA$ where B is the magnetic induction and A is the cross-sectional area of the flux tube. Collecting this information together, the four conserved quantities are

$$\mu = T/B \quad (2a)$$

$$J = T^{1/2}L \quad (2b)$$

$$N = n A L \quad (2c)$$

$$B = B A. \quad (2d)$$

Expressions (2a)–(2d) are four expressions in five unknowns: T , B , L , A , and n . The five unknowns are not conserved quantities; they are variables. Algebraically, using three of the expressions to eliminate the variables A , L , and B leaves one expression which has the two variables n and T :

$$N/B \mu J = n/T^{3/2}. \quad (3)$$

The left-hand side of expression (3) is composed entirely of conserved quantities, so both sides of expression (3) are conserved. Expression (3) is interpreted as follows. N/B is the number of particles per unit flux in the flux tube. Thus the left-hand side $N/B\mu J$ is the number density of $(\mu J)^{-1}$ in the flux tube, where the number density is the number of particles per unit flux instead of the number per unit volume. Hence $N/B\mu J$ is the amount of $(\mu J)^{-1}$ per unit flux

in a flux tube. Since μ is an adiabatic invariant and J is an adiabatic invariant, the quantity $(\mu J)^{-1}$ is also an adiabatic invariant; it can be called a hybrid adiabatic invariant.

[12] Taking both sides of expression (3) to the $2/3$ power and recognizing from expression (1) that $T/n^{2/3} = S$, expression (3) becomes

$$S = (\mu J B / N)^{2/3}, \quad (4)$$

where the specific entropy S is written in terms of single particle motions in a collisionless plasma rather than fluid variables. In expression (4) the first and second adiabatic invariants μ and J pertain to thermal particles in the population. According to expression (4), the specific entropy S can be interpreted as $S^{-3/2}$ being the density of the hybrid adiabatic invariant $(\mu J)^{-1}$ per unit flux.

2.2. Specific Entropy for Relativistic Maxwellians

[13] For a hot plasma, there are relativistic corrections to the expression $S = T/n^{2/3}$ for the specific entropy. The specific entropy (entropy per particle) S is related to the Boltzmann H function $H = \int f \log(f) d^3v$ as $\log(S^{3/2}) = -k_B H$ [cf. Boyd and Sanderson, 1969, section 10–8]. For a non-relativistic Maxwellian distribution function $f(v)$, the integral $\int f \log(f) d^3v$ is performed to yield $S = T/n^{2/3}$ [cf. Fitts and Mucci, 1962; Chapman and Cowling, 1953, section 4.2]. For a relativistic Maxwellian distribution $f(p)$ the H function $H = \int f \log(f) d^3p$ is related to the entropy in the same fashion $\log(S^{3/2}) = -k_B H$ [Alvarez, 1979; Escobedo *et al.*, 2003; Kaniadakis, 2009]. For a relativistic Maxwellian distribution $f(E) = n (c/4\pi m_e k_B T^2) [\alpha e^{\alpha} K_2(\alpha)]^{-1} \exp(-E/k_B T)$ [Cayton *et al.*, 1989] of kinetic energy E , the integral $\int f \log(f) d^3p$ is performed to yield

$$S = F^{-2/3} n^{-2/3} \quad (5)$$

for the specific entropy, where the function F is

$$F(\alpha) = (\alpha/K_2(\alpha)) \exp[-\alpha K_3(\alpha)/K_2(\alpha)] \quad (6)$$

with $\alpha = m_e c^2/k_B T$ and where K_2 and K_3 are modified Bessel functions. The specific entropy expression (5) can be approximated (to within 3.2%) by the expression

$$S \approx T \left(1 + (T/137.9)^{1.275} \right)^{1/1.275} n^{-2/3} \quad (7)$$

with T expressed in units of keV. Expression (7) varies as $S \propto T^1$ at low temperature (nonrelativistic) and varies as $S \propto T^2$ at high temperature (fully relativistic).

[14] The approximation (expression (7)) to the specific entropy S can also be obtained from expression (4) for the adiabatic-invariant density per unit flux by (1) retaining the relativistic expressions $\mu = p_{\perp}^2/B$ and $J = p_{\parallel}L$ for the μ and J adiabatic invariants [e.g., Northrop and Teller, 1960; Alfvén and Falthammar, 1963] and (2) using the facts that the mean kinetic energy $\langle E \rangle = m_e v^2/2$ of a distribution is $\langle E \rangle = 3/2 k_B T$ for nonrelativistic electrons $k_B T \ll m_e c^2$ and that the mean kinetic energy $\langle E \rangle = (\langle \gamma \rangle - 1)m_e c^2$ is $\langle E \rangle = 3 k_B T$ for fully relativistic electrons $k_B T \gg m_e c^2$ [e.g., Wienke, 1975; Wei-Ke *et al.*, 2005]. Hence the interpretation in section 2.1 of S as the density of a hybrid adiabatic invariant

$(\mu\text{J})^{-1}$ per unit flux holds relativistically, with S given by expression (5) or expression (7).

3. The Specific Entropy of the Outer Electron Radiation Belt at Geosynchronous Orbit

[15] The energetic electrons at geosynchronous orbit are measured by the Synchronous Orbit Particle Analyzer (SOPA) [Belian et al., 1992; Cayton and Belian, 2007] on board seven satellites in geosynchronous orbit (6.6 R_E). The SOPAs measure fluxes of electrons in the energy range $\sim 30 \text{ keV}$ to $> 2 \text{ MeV}$ every 10 s. In the current study, the spin-averaged counting rates for each electron energy channel are modeled as linear combinations of two Maxwellian components plus a nonelectron “background” contribution; minimizing the squared deviations between the observed and model counting rates summed over 10 electron channels yields the best fit two-Maxwellian spectra (see Cayton and Belian [2007] for full details). Spin-averaged count rates (obtained by averaging over the spacecraft spin) are fit rather than omnidirectional count rates (obtained by integrating over the pitch angle distribution); analysis has shown that spin-averaged and omnidirectional quantities are almost identical for the energetic electrons measured by SOPA at geosynchronous orbit (R. Friedel, private communication, 2009). Cayton et al. [1989] found that relativistic bi-Maxwellians were excellent fits to the omnidirectional electron fluxes at geosynchronous orbit; Pierrard and Lemaire [1996] drew similar conclusions for the outer electron radiation belt away from geosynchronous orbit. The assumption of isotropy is implicit in the present data analysis; future analysis will produce densities and temperatures of the electron bi-Maxwellians as functions of pitch angle. The bi-Maxwellian fitting describes two populations of electrons, a “soft” population of electrons with a temperature of $\sim 30 \text{ keV}$ and a “hard” population of electrons with a temperature of $\sim 150 \text{ keV}$. The “soft” population is the suprathermal tail of the electron plasma sheet whose appearance at geosynchronous orbit is associated with substorm injections [Lezniak et al., 1968; Cayton et al., 1989; Birn et al., 1998]. The hard component is the outer electron radiation belt [Cayton et al., 1989; Belian et al., 1996]. As an aside, note that Johnson and Wing [2009] used (nonrelativistic) bi-Maxwellian fits to the ion plasma sheet population to study separately the specific entropy of the ion plasma sheet core distribution and of the ion plasma sheet halo distribution.

[16] From the measured count rates, the temperatures and densities of the hard and soft components are determined from functional fits every 10 s from each satellite. In this paper only the hard component density and temperature are utilized. To reduce the influence of outliers when the fits are noisy and to produce a more manageable sized data set, median values of the density and temperature are calculated for every 30 min of data [cf. Denton et al., 2010]. Data from the declining phase years 1989–2008 are used [cf. Denton et al., 2010]. This results in 955,527 half-hour median values of temperature and density, which is equivalent to 54.5 satellite years of data. The specific entropy $S = F^{-2/3} n^{-2/3}$ (expressions (5) and (7)) of the outer electron radiation belt at geosynchronous orbit will be calculated from these half-hour median temperature and density measurements.

[17] In Figure 2 the number density n , temperature T , and specific entropy $S = F^{-2/3} n^{-2/3}$ of the outer electron radiation

belt at geosynchronous orbit local midnight are binned. Only measurements within $\pm 1 \text{ h}$ of local midnight are used. In Figure 2 (top), $\log_{10}(n)$ is binned. Note the asymmetry in the distribution, with a maximum n value of $n \sim 1 \times 10^{-4} \text{ cm}^{-3}$ and a low-density tail extending below $n \sim 1 \times 10^{-5} \text{ cm}^{-3}$. The mean value \pm standard deviation of the distribution of n values is $n = 3.4 \times 10^{-4} \pm 2.4 \times 10^{-4} \text{ cm}^{-3}$, as noted in the plot. In Figure 2 (middle) the quantity $\log_{10}(T)$ of the outer electron radiation belt at geosynchronous midnight is binned, with T measured in keV. Note that this distribution is symmetric and varies by less than 1 decade. The mean value \pm standard deviation of the temperature distribution is $T = 139 \pm 45 \text{ keV}$. In Figure 2 (bottom) the quantity $\log_{10}(S)$ of the outer electron radiation belt at geosynchronous midnight is binned, with $S = F^{-2/3} n^{-2/3}$ (expression (5)) measured in units of eV cm^2 . Note that this distribution is asymmetric with a high- S tail that corresponds to the low- n tail of Figure 2 (top) (i.e., $\log_{10}(S) = -2/3 \log_{10}(F) - 2/3 \log_{10}(n)$). The mean value \pm standard deviation of the distribution of S values at geosynchronous orbit local midnight is $S = 8.4 \times 10^7 \pm 1.4 \times 10^8 \text{ eV cm}^2$. (The standard deviation exceeds the mean value owing to the high-entropy tail of the distribution associated with low-density events.)

[18] In Figure 3 the measured values of the specific entropy (expression (5)) of the outer electron radiation belt are plotted as a function of local time around geosynchronous orbit. Each gray point is the median value for $1/2 \text{ h}$ of measurements and the red points are 10,000-point running logarithmic averages of the gray points. As can be seen by the red points, there is no strong trend to the specific entropy S versus local time. Note, however, that there are strong local time trends in the number density n and temperature T of the outer electron radiation belt at geosynchronous orbit [cf. Denton et al., 2010, Figure 3], which are owed to the fact that geosynchronous local noon samples a deeper outer electron radiation belt population (with a higher n and higher T) than does geosynchronous orbit midnight [Hones, 1963; Pfitzer et al., 1969; Borovsky and Denton, 2010a]. Nevertheless, the specific entropy $S = F^{-2/3} n^{-2/3}$ of these two radial populations is quite similar.

4. The Specific Entropy of the Energetic Electrons in the Magnetotail

[19] Omnidirectional energetic electron measurements in the energy range ~ 0.1 – 6 MeV on 12 Global Positioning System (GPS) satellites are used to determine the number density and temperature of the energetic electron population in the Earth's magnetotail. The measurements are from the years 2006–2010. The instrumentation used is the Burst Detection Dosimeter (BDD-IIR) [Cayton et al., 1998, 2010] operating on two early satellites and the Combined X-ray and Dosimeter (CXD) [Distel et al., 1999; Cayton et al., 2010] instruments operating on 10 later satellites, with modeling of the instrument response by Tuszezski et al. [2002]. Densities and temperatures of the electrons are obtained from relativistic Maxwellian fits to the count rates (cf. Denton and Cayton, submitted manuscript, 2011). The count rate corrected for dead time is modeled as a sum of two contributions, nonelectron background counts plus counts that result from a spectrum of incident electrons. Values for the density and temperature of the electrons are

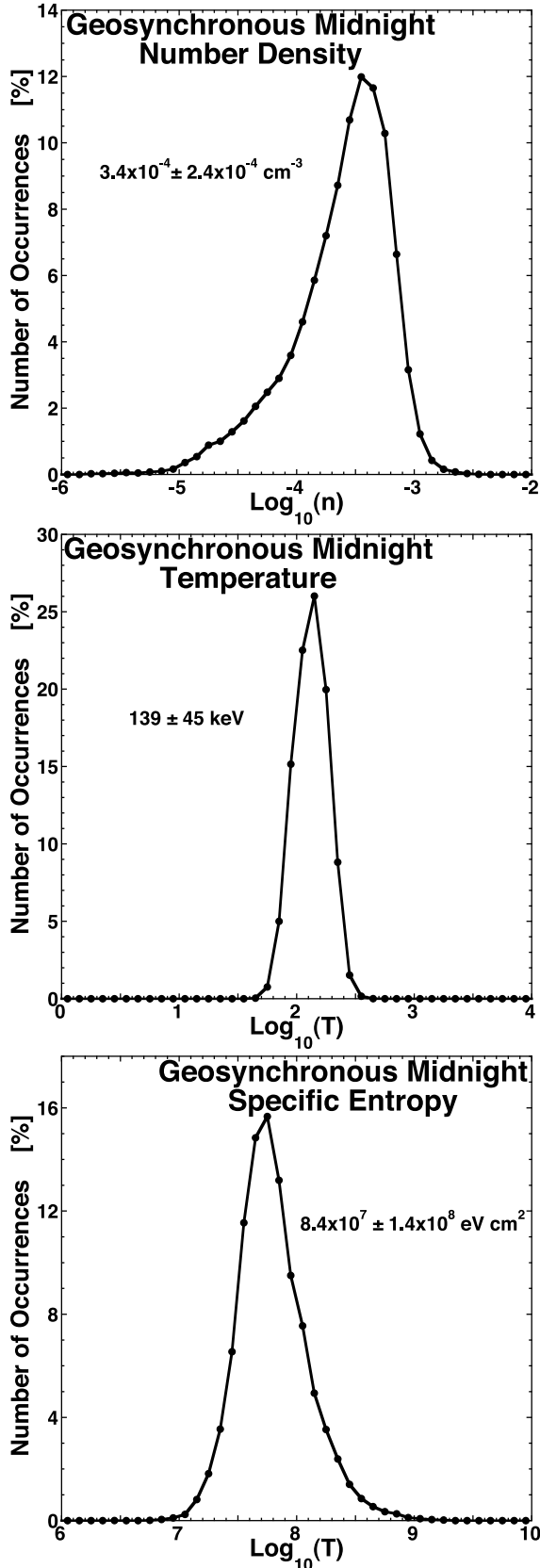


Figure 2. The occurrence distributions for $\log_{10}(n)$, $\log_{10}(T)$, and $\log_{10}(S)$ for the outer electron radiation belt at geosynchronous orbit local midnight as determined from SOPA energetic electron measurements.

inferred by least squares fits of relativistic Maxwellians, minimizing the sum of the squared deviations between the sets of true and predicted counting rates. The analysis is optimized for the energies $\sim 0.1\text{--}1.0$ MeV.

[20] The magnetotail energetic electron population will be measured by the “off equatorial” GPS spacecraft (similar to the measurements of the magnetotail ion plasma sheet by the DMSP spacecraft [Wing and Newell, 1998], but not as extreme). In general the energetic electron population in the magnetotail is quasi-isotropic [Hones *et al.*, 1968; Retzler and Simpson, 1969; Sarris *et al.*, 1976], so it is easily detected by the off-equatorial GPS spacecraft and Liouville’s theorem preserves the number density and the temperature of the energetic electron population along the flux tube away from the equator.

[21] Mapping of the magnetic field line from the GPS spacecraft to the equatorial (minimum B) plane is performed with the T89 [Tsyganenko, 1989; Peredo *et al.*, 1993] magnetic field model using an IGRF internal field (see also Denton and Cayton, submitted manuscript, 2011). The K_p value for the T89 model is set to K_p = 2. Using the magnetic field models the value B_{sat} of the magnetic field at the GPS satellite is estimated. Computationally tracing the magnetic field line through the satellite, the bounce invariant $\int (1 - B/B_{\text{sat}})^{1/2} ds$ is integrated for a particle mirroring at the satellite. Using the asymptotic expansion of Hilton [1971], an approximate value for McIlwain’s L parameter [McIlwain, 1961] is obtained. This L parameter is used as a measure of the downtail distance that the GPS satellite maps to. Only measurements that map to greater than 10 R_E downtail (L > 10) are used and only measurements made within ± 1 h of local midnight are used. The choice of L = 10 as an inner boundary is somewhat

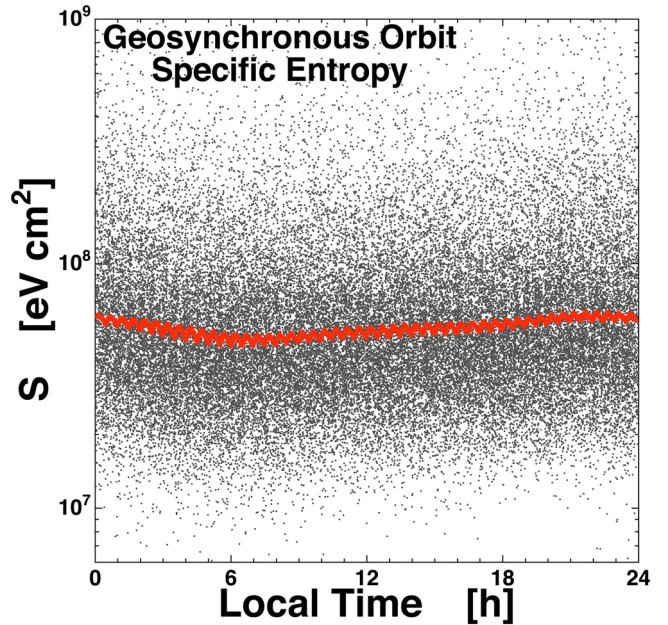


Figure 3. For 955,527 half-hour measurements, the specific entropy of the outer electron radiation belt at geosynchronous orbit is plotted as a function of the local time at which the measurement was obtained. The gray points are the individual measurements (every 20th point plotted), and the red points are 10,000-point running averages of the gray points.

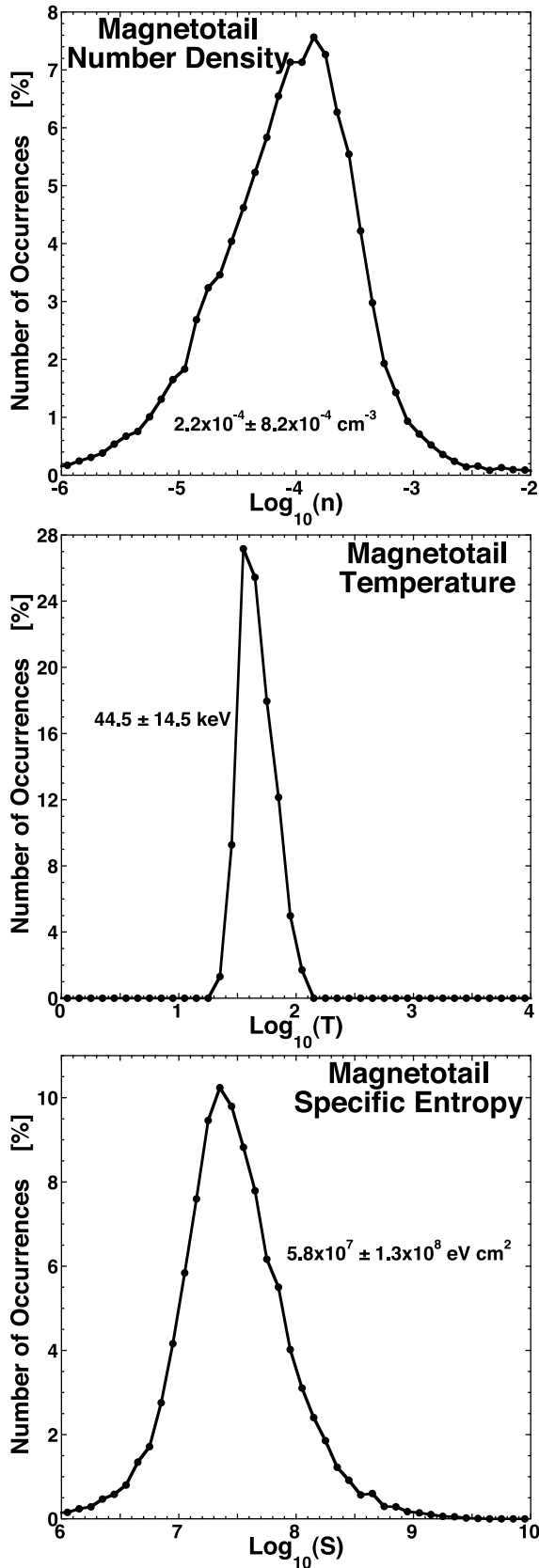


Figure 4. The occurrence distributions for $\log_{10}(n)$, $\log_{10}(T)$, and $\log_{10}(S)$ for the energetic electron population in the magnetotail as determined from GPS energetic electron measurements.

arbitrary; $L > 10$ was chosen to be beyond the dipolar portion of the magnetosphere.

[22] In Figure 4 the occurrence distributions of the number density n , temperature T , and specific entropy $S = F^{-2/3} n^{-2/3}$ of the energetic electron population of the magnetotail as viewed by GPS are plotted. (Again, only measurements within ± 1 h of local midnight and $L > 10$ are included in the binning.) In Figure 4, $\log_{10}(n)$ is binned. Note that the $\log_{10}(n)$ distribution is slightly asymmetric, with a low-density tail. (This is similar to the $\log_{10}(n)$ distribution at geosynchronous orbit displayed in Figure 2 (top).) The mean value \pm standard deviation of the distribution of n values for the magnetotail is $n = 2.2 \times 10^{-4} \pm 8.2 \times 10^{-4} \text{ cm}^{-3}$, as noted in the plot. In Figure 4 (middle) the quantity $\log_{10}(T)$ of the energetic electron population of the magnetotail is binned, with T measured in keV. Note that this distribution is symmetric and varies by less than 1 decade. (This is similar to the $\log_{10}(T)$ distribution at geosynchronous orbit displayed in Figure 2 (middle).) The mean value \pm standard deviation of the temperature distribution for the magnetotail is $T = 44.5 \pm 14.5 \text{ keV}$, as noted on the plot. In Figure 4 (bottom) the quantity $\log_{10}(S)$ of the energetic-electron population of the magnetotail is binned, with $S = F^{-2/3} n^{-2/3}$ (expression (5)) measured in units of eV cm^2 . Note that this distribution is asymmetric with a high-S tail that corresponds to the low- n tail of Figure 4 (top) (as is the case for the outer electron radiation belt at geosynchronous orbit, plotted in Figure 2 (bottom)). The mean value \pm standard deviation of the distribution of S values for the energetic electron population of the magnetotail is $S = 5.8 \times 10^7 \pm 1.3 \times 10^8 \text{ eV cm}^2$, as noted on the plot. Denton and Cayton (2011) found that the number density n and temperature T of this magnetotail energetic population both decrease with increasing distance downtail, as determined from the T89 mapping of the GPS measurements.

5. Entropy Mapping Between the Magnetotail and Geosynchronous Orbit

[23] The entropy mapping of the outer electron radiation belt between the magnetotail and geosynchronous orbit is explored in Figure 5. Here, for various particle populations measurements of temperature T are plotted as a function of measurements of number density n . Constant values of the nonrelativistic specific entropy $S = T/n^{2/3}$ given by expression (1) are indicated by the diagonal gray dashed lines in the plot and constant values of the relativistic specific entropy $S = F^{-2/3} n^{-2/3}$ given by expression (7) are indicated by the orange curves in the plot. SOPA measurements of the outer electron radiation belt at geosynchronous orbit midnight are plotted as green points in the upper left portion of Figure 5. The median value of these points is indicated by a white circle with a green dot. GPS measurements of the energetic electrons in the magnetotail are split into two groups according to downtail distance, a group with $10 < L < 22$ representing the near-Earth magnetotail and a group with $L > 22$ representing the distant magnetotail. The GPS measurements for the near-Earth magnetotail are plotted as blue points in the upper left portion of Figure 5 and the GPS measurements for the distant magnetotail are plotted as red points. The median values of these two groups are indicated by white circles with a blue dot and a red dot.

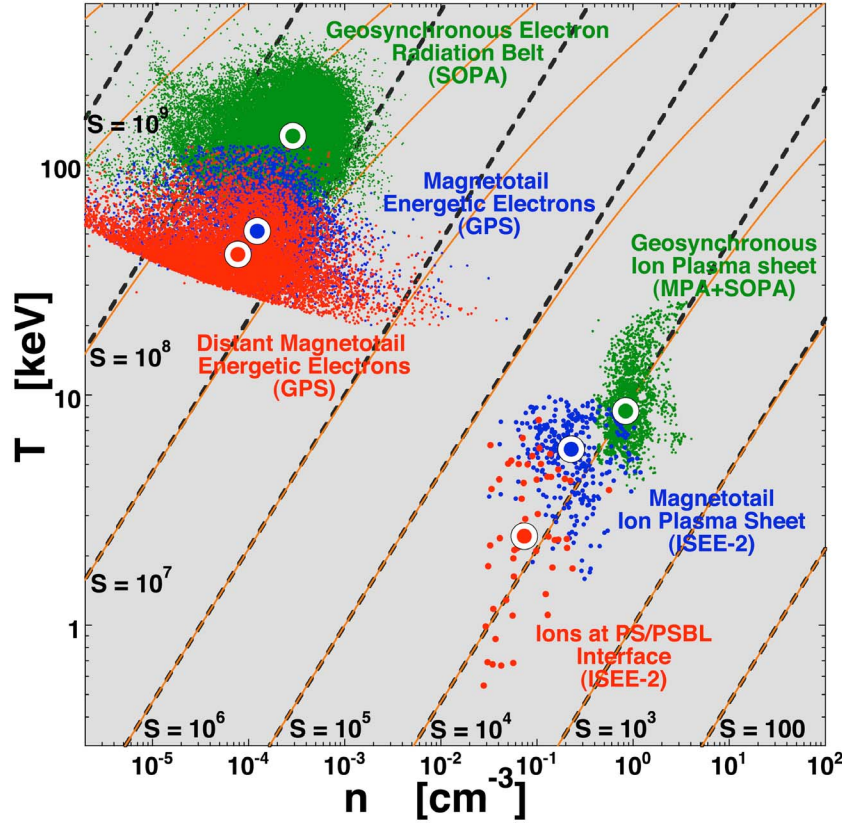


Figure 5. Temperature T is plotted as a function of number density n for measurements of the outer electron radiation belt at geosynchronous orbit midnight (green points, upper left), energetic electrons in the magnetotail at $10 < L < 22$ (blue points, upper left), energetic electrons in the magnetotail at $L > 22$ (red points, upper left), the ion plasma sheet at geosynchronous orbit local midnight (green points, lower right), the ion plasma sheet in the $11-22 R_E$ downtail distance range (blue points, lower right), and the ion plasma sheet in the distant tail (red points, lower right). Median values of the six populations are indicated by the white circles with colored dots. The black diagonal lines are curves of constant nonrelativistic specific entropy $S = T/n^{2/3}$ labeled in units of eV cm² and the orange curves are curves of constant relativistic specific entropy $S = F^{-2/3} n^{-2/3}$.

[24] In the lower right portion of Figure 5, density-temperature measurements of the Earth's ion plasma sheet are plotted, after Plate 1 of Borovsky *et al.* [1998b] (see also Figure 6 of Wing and Johnson [2009] and Figure 3 of Johnson and Wing [2009]); the green points are MPA-SOPA measurements at geosynchronous orbit midnight, the blue points are ISEE-2 measurements from neutral sheet crossings in the magnetotail from $11 R_E < d < 22 R_E$ downtail distance, and the red points are ISEE-2 measurements from the outer edge of the magnetotail plasma sheet which map to the distant tail. Median values for the three populations are indicated by white circles with colored dots. Note that all three ion plasma sheet populations have approximately the same value of S . The interpretation [cf. Borovsky *et al.*, 1998b] is that the three populations are the same population seen at three locations as the ions convect, with n and T adiabatically increasing as the population migrates from the distant tail (red) to the near-Earth tail (blue) into the dipole (green).

[25] A similar interpretation for the red, blue, and green points of the outer electron radiation belt in the upper left portion of Figure 5 is that they are the same population. The interpretation would be either (1) the energetic electrons are

adiabatically heated as they move from the magnetotail to geosynchronous orbit or (2) that the energetic electrons are adiabatically cooled as they move from the dipole into the magnetotail. Scenario 1 would indicate that the magnetotail energetic electrons are a source population for the outer electron radiation belt; scenario 2 would indicate that the energetic electrons of the magnetotail are leakage from the outer electron radiation belt. More investigation is required to discern whether scenario 1 or scenario 2 is operating.

6. Discussion

[26] Specific entropy evidence has been presented that the energetic electron population in the magnetotail is the same population as the outer electron radiation belt at geosynchronous orbit. Two questions about this can be asked: (1) Is adiabatic motion between the magnetotail and geosynchronous orbit possible for energetic electrons and (2) if so, how much change in density and temperature is expected in going between the two locations? These two questions are discussed in the following two paragraphs.

[27] Two possible means of transport between the magnetotail and geosynchronous orbit are via electric field drift or via radial diffusion. If energetic electrons are transported between the magnetotail and geosynchronous orbit by electric field drift [e.g., *Birn et al.*, 1998, 2000; *Fok et al.*, 2001], then the transport should be adiabatic (in that the μ and J invariants are conserved) provided that the electric and magnetic fields in the magnetosphere do not vary on timescales comparable to or faster than the electron bounce period. The energetic electron bounce period in the magnetosphere is a few seconds or less, even in the magnetotail. Observations of temporal changes in nightside electric fields in the magnetosphere show timescales for change of a minute or longer [cf. *Aggson et al.*, 1983, Figure 4; *Roux et al.*, 1991, Figure 2; *Pedersen*, 1992, Figure 1 of; *Pedersen and Escoubet*, 1994, Figure 2; *Kozelova et al.*, 2000, Figures 1 and 2]. Similar timescales are seen for temporal changes in the nightside magnetic field in the magnetosphere [cf. *Aggson et al.*, 1983, Figure 4; *Kremser et al.*, 1988, Figures 1 and 2; *Takahashi et al.*, 1987, Figure 1; *Lopez et al.*, 1990, Figure 14; *Williams et al.*, 1990, Figure 1; *Pudovkin*, 1991, Figure 7; *Ohtani et al.*, 1991, Figures 1 and 2; *Lui et al.*, 1992, Table 1; *Lopez et al.*, 1993, Figure 5; *Rastinkangas et al.*, 1994, Figure 4]. If energetic electrons are transported between the magnetotail and geosynchronous orbit by inward or outward radial diffusion, then the transport should be adiabatic (in that the μ and J invariants are conserved) if the radial diffusion is driven by fluctuations with timescales longer than the bounce periods of energetic electrons. In the quasi-dipolar regions of the magnetosphere radial diffusion is thought to be driven by small-amplitude ULF fluctuations and is thought to conserve μ and J for energetic electrons [*Schulz and Eviatar*, 1969; *Walt*, 1971; *Sarris et al.*, 2006]. In the magnetotail radial diffusion could be driven by the large-amplitude MHD turbulence fluctuations of the plasma sheet [*Borovsky et al.*, 1997; *Borovsky and Funsten*, 2003; *Vörös et al.*, 2004; *Weygand et al.*, 2005; *Stepanova et al.*, 2005, 2009; *El-Alaoui et al.*, 2010]. In this turbulence, conservation of the J invariant depends on the gradient and curvature drift velocity of an energetic electron compared with the approximately $1.5 R_E$ correlation length of the turbulence across the magnetic field. Preliminary particle orbit calculations in nonturbulent magnetic field models (J. Birn, private communication, 2011) indicates that electrons should move through a turbulence correlation length in a time that is longer than their bounce times, indicating that their adiabaticity should be conserved while radially diffusing in the turbulence. As noted in Figures 2 (bottom) and 4 (bottom), the measured mean values of $S = F^{-2/3} n^{-2/3}$ for energetic electrons tend to be about 45% higher at geosynchronous orbit midnight than in the magnetotail. If this measured difference in the specific entropy S is accurate, then this would be consistent with a nonadiabatic heating of the electrons as they move from the magnetotail to geosynchronous orbit or a nonadiabatic cooling as they move from geosynchronous orbit to the magnetotail. Nonadiabatic heating could be caused, for instance, by wave-particle interactions with plasma waves [e.g., *Summers and Ma*, 2000; *Albert*, 2004; *Horne et al.*, 2005, 2007]; nonadiabatic cooling could be caused, for instance, by energy-dependent electron loss.

[28] As can be seen in Figure 5, the amount of change in n and T of the energetic electrons between the magnetotail and

geosynchronous orbit midnight is about the same for the energetic electrons (upper left of Figure 5) and the ion plasma sheet ions (lower right of Figure 5); in both cases the number density at geosynchronous orbit is about a factor of 4 higher than the number density in the magnetotail. It has been noted by *Borovsky et al.* [1998b] that the amount of change in n and T seen for the ion plasma sheet is much less than expected from the simple use of static magnetic field models of the magnetosphere; it was argued that in time-dependent magnetospheres with reconnection the specific entropy could be conserved [cf. *Borovsky and Hesse*, 2007] while the total entropy (integral of the specific entropy over the volume of a flux tube) was not conserved [cf. *Birn et al.*, 2006], yielding adiabatic behavior with smaller-than-expected values for the compression of n . (For an example of this conservation of specific entropy and nonconservation of total entropy in the magnetotail, compare Figures 4a and 4d of *Johnson and Wing* [2009].) The case could be the same for the energetic electrons since adiabaticity appears to hold between geosynchronous orbit and the magnetotail and since the same amount of density change is seen between the two locations.

7. Summary

[29] Using number density n and temperature T measurements the specific entropy values $S = T/n^{2/3}$ of the outer electron radiation belt at geosynchronous orbit and of the energetic electron population of the magnetotail are determined. The specific entropies of these two populations statistically match. This match indicates that the outer electron radiation belt at geosynchronous orbit and the energetic electrons in the magnetotail are probably the same population, either (1) adiabatically heating moving earthward or (2) adiabatically cooling moving tailward. In case 1 the energetic electrons of the magnetotail would be a source population for the outer electron radiation belt in the dipole. In that case a question arises as to the origin of those energetic electrons in the magnetotail. In case 2 the energetic electrons of the magnetotail are electrons leaked from the outer electron radiation belt in the dipole and are electrons being exhausted from the Earth's magnetosphere. In that case a question arises as to the origin of the outer electron radiation belt electrons.

[30] **Acknowledgments.** The authors wish to thank Evan Noveroske for providing the BDD and CXD data files, to thank Mick Denton for preparing data sets, and to thank Joachim Birn and Mick Denton for stimulating conversations. This work was supported by the NASA Living with a Star TR&T Program and by the U.S. Department of Energy.

[31] Masaki Fujimoto thanks the reviewers for their assistance in evaluating this paper.

References

- Aggson, T. L., J. P. Heppner, and N. C. Maynard (1983), Observations of large magnetospheric electric fields during the onset phase of a substorm, *J. Geophys. Res.*, 88, 3981, doi:10.1029/JA088iA05p03981.
- Albert, J. M. (2004), Using quasi-linear diffusion to model acceleration and loss from wave-particle interactions, *Space Weather*, 2, S09S03, doi:10.1029/2004SW000069.
- Alfvén, H., and C.-G. Falthammar (1963), *Cosmical Electrodynamics*, Oxford Univ. Press, New York.
- Alvarez, E. (1979), The relativistic scalar entropy, *Phys. Lett. A*, 70, 363.
- Baumjohann, W. (1993), The near-Earth plasma sheet: An AMPTE/IRM perspective, *Space Sci. Rev.*, 64, 141, doi:10.1007/BF00819660.

- Baumjohann, W., and G. Paschmann (1989), Determination of the polytropic index in the plasma sheet, *Geophys. Res. Lett.*, **16**, 295, doi:10.1029/GL016i004p00295.
- Belian, R. D., G. R. Gisler, T. Cayton, and R. Christensen (1992), High-Z energetic particles at geosynchronous orbit during the great solar proton event series of October 1989, *J. Geophys. Res.*, **97**, 16,897, doi:10.1029/92JA01139.
- Belian, R. D., T. E. Cayton, R. A. Christiansen, J. C. Ingraham, M. M. Meier, G. D. Reeves, and A. J. Lazarus (1996), Relativistic electrons in the outer-zone: An 11 year cycle; Their relation to the solar wind, in *AIP Proceedings 383 Workshop on the Earth's Trapped Particle Environment*, edited by G. D. Reeves, pg. 13, Am. Inst. of Phys., Woodbury N. Y.
- Bernstein, I. B., E. A. Friemen, M. D. Kruskal, and R. M. Kulrud (1958), An energy principle for hydromagnetic stability problems, *Proc. R. Soc. London, Ser. A*, **244**, 17, doi:10.1098/rspa.1958.0023.
- Bezrodnykh, N. P., E. G. Berezhko, I. Y. Plotnikov, Y. G. Shafer, E. I. Morozova, and N. F. Pisarenko (1984a), High-energy electron fluxes close to the magnetopause and in a geosynchronous orbit. Analysis of experimental results and generation mechanism, *Bull. Acad. Sci. USSR Phys. Ser.*, **48**, 101.
- Bezrodnykh, N. P., E. G. Berezhko, E. I. Morozova, N. F. Pisarenko, I. Y. Plotnikov, and Y. G. Shafer (1984b), Bursts of relativistic electrons on the magnetopause and in the outer radiation belt, *Geomagn. Aeron.*, **24**, 666.
- Bezrodnykh, E., I. Morozova, and Y. G. Shafer (1987), Effect of large-scale disturbances of the solar wind on the dynamics of relativistic electrons of the outer radiation belt, *Cosmic Res., Engl. Transl.*, **25**, 56.
- Birn, J., and K. Schindler (1983), Self-consistent theory of three-dimensional convection in the geomagnetic tail, *J. Geophys. Res.*, **88**, 6969, doi:10.1029/JA088iA09p06969.
- Birn, J., M. F. Thomsen, J. E. Borovsky, G. D. Reeves, D. J. McComas, R. D. Belian, and M. Hesse (1998), Substorm electron injections: Geosynchronous observations and test particle simulations, *J. Geophys. Res.*, **103**, 9235, doi:10.1029/97JA02635.
- Birn, J., M. F. Thomsen, J. E. Borovsky, G. D. Reeves, and M. Hesse (2000), Particle acceleration in the dynamic magnetotail, *Phys. Plasmas*, **7**, 2149, doi:10.1063/1.874035.
- Birn, J., M. Hesse, and K. Schindler (2006), Entropy conservation in simulations of magnetic reconnection, *Phys. Plasmas*, **13**, 092117, doi:10.1063/1.2349440.
- Birn, J., M. Hesse, K. Schindler, and S. Zaharia (2009), The role of entropy in magnetotail dynamics, *J. Geophys. Res.*, **114**, A00D03, doi:10.1029/2008JA014015.
- Borovsky, J. E. (2008a), The flux tube texture of the solar wind: Strands of the magnetic carpet at 1 AU, *J. Geophys. Res.*, **113**, A08110, doi:10.1029/2007JA012684.
- Borovsky, J. E. (2008b), The rudiments of a theory of solar-wind/magnetosphere coupling derived from first principles, *J. Geophys. Res.*, **113**, A08228, doi:10.1029/2007JA012646.
- Borovsky, J. E., and M. H. Denton (2009), Electron loss rates from the outer electron radiation belt caused by the filling of the outer plasmisphere: The calm before the storm, *J. Geophys. Res.*, **114**, A11203, doi:10.1029/2009JA014063.
- Borovsky, J. E., and M. H. Denton (2010a), On the heating of the outer radiation belt to produce high fluxes of relativistic electrons: Measured heating rates at geosynchronous orbit for high-speed-stream-driven storms, *J. Geophys. Res.*, **115**, A12206, doi:10.1029/2010JA015342.
- Borovsky, J. E., and M. H. Denton (2010b), Solar-wind turbulence and shear: A superposed-epoch analysis of corotating interaction regions at 1 AU, *J. Geophys. Res.*, **115**, A10101, doi:10.1029/2009JA014966.
- Borovsky, J. E., and M. H. Denton (2011), A survey of the anisotropy of the outer electron radiation belt during high-speed-stream-driven storms, *J. Geophys. Res.*, **116**, A05201, doi:10.1029/2010JA016151.
- Borovsky, J. E., and H. O. Funsten (2003), MHD turbulence in the Earth's plasma sheet: Dynamics, dissipation, and driving, *J. Geophys. Res.*, **108**(A7), 1284, doi:10.1029/2002JA009625.
- Borovsky, J. E., and S. P. Gary (2011), Electron-ion Coulomb scattering and the electron Landau damping of Alfvén waves in the solar wind, *J. Geophys. Res.*, doi:10.1029/2010JA016403, in press.
- Borovsky, J. E., and P. J. Hansen (1991), Breaking the first adiabatic invariants of charged particles in time-dependent magnetic fields: Computer simulations and theory, *Phys. Rev. A*, **43**, 5605, doi:10.1103/PhysRevA.43.5605.
- Borovsky, J. E., and M. Hesse (2007), The reconnection of magnetic fields between plasmas with different densities: Scaling relations, *Phys. Plasmas*, **14**, 102309, doi:10.1063/1.2772619.
- Borovsky, J. E., C. K. Goertz, and G. Joyce (1981), Magnetic pumping of particles in the outer Jovian magnetosphere, *J. Geophys. Res.*, **86**, 3481, doi:10.1029/JA086iA05p03481.
- Borovsky, J. E., R. C. Elphic, H. O. Funsten, and M. F. Thomsen (1997), The Earth's plasma sheet as a laboratory for flow turbulence in high-beta MHD, *J. Plasma Phys.*, **57**, 1, doi:10.1017/S0022377896005259.
- Borovsky, J. E., M. F. Thomsen, D. J. McComas, T. E. Cayton, and D. J. Knipp (1998a), Magnetospheric dynamics and mass flow during the November 1993 storm, *J. Geophys. Res.*, **103**, 26,373, doi:10.1029/97JA03051.
- Borovsky, J. E., M. F. Thomsen, R. C. Elphic, T. E. Cayton, and D. J. McComas (1998b), The transport of plasma sheet material from the distant tail to geosynchronous orbit, *J. Geophys. Res.*, **103**, 20,297, doi:10.1029/97JA03144.
- Boyd, T. J. M., and J. J. Sanderson (1969), *Plasma Dynamics*, Barnes and Noble, New York.
- Brech, B., W. H. Matthaeus, S. R. Cranmer, J. C. Kasper, and S. Oughton (2009), Electron and proton heating by solar wind turbulence, *J. Geophys. Res.*, **114**, A09103, doi:10.1029/2009JA014354.
- Burlaga, L. F., W. H. Mish, and Y. C. Whang (1990), Coalescence of recurrent streams of different sizes and amplitudes, *J. Geophys. Res.*, **95**, 4247, doi:10.1029/JA095iA04p04247.
- Burton, M. E., M. Neugebauer, N. U. Crooker, R. von Steiger, and E. J. Smith (1999), Identification of trailing edge solar wind stream interfaces: A comparison of Ulysses plasma and compositional measurements, *J. Geophys. Res.*, **104**, 9925.
- Cayton, T. E., and R. D. Belian (2007), Numerical modeling of the synchronous orbit particle analyzer, *Rep. LA-14335*, Los Alamos Natl. Lab., Los Alamos, N. M.
- Cayton, T. E., R. D. Belian, S. P. Gary, T. A. Fritz, and D. N. Baker (1989), Energetic electron components at geosynchronous orbit, *Geophys. Res. Lett.*, **16**, 147, doi:10.1029/GL016i002p00147.
- Cayton, T. E., D. M. Drake, K. M. Spencer, M. Herrin, T. J. Wehenr, and R. C. Reedy (1998), Description of the BDD-IIR: Electron and proton sensors on the GPS, *Tech. Rep. LA-UR-98-1162*, Los Alamos Natl. Lab., Los Alamos, N. M.
- Cayton, T. E., Y. Chen, R. H. W. Friedel, and R. M. Kippen (2010), Analysis of electron and proton environmental data for medium-Earth orbit (2000–present), *Tech. Rep. LA-UR-10-4234*, Los Alamos Natl. Lab., Los Alamos, N. M.
- Chapman, S., and T. G. Cowling (1953), *The Mathematical Theory of Non-Uniform Gases*, Cambridge Univ. Press, London.
- Comfort, R. H. (1986), Plasmasphere thermal structure as measured by ISEE-1 and DE-1, *Adv. Space Res.*, **6**(3), 31, doi:10.1016/0273-1177(86)90314-5.
- Crooker, N. U., M. E. Burton, G. L. Siscoe, S. W. Kahler, J. T. Gosling, and E. J. Smith (1996), Solar wind streamer belt structure, *J. Geophys. Res.*, **101**, 24,331, doi:10.1029/96JA02412.
- Denton, M. H., M. F. Thomsen, H. Korth, S. Lynch, J. C. Zhang, and M. W. Liemohn (2005), Bulk plasma properties at geosynchronous orbit, *J. Geophys. Res.*, **110**, A07223, doi:10.1029/2004JA010861.
- Denton, M. H., J. E. Borovsky, and T. E. Cayton (2010), A density-temperature description of the outer electron radiation belt during geomagnetic storms, *J. Geophys. Res.*, **115**, A01208, doi:10.1029/2009JA014183.
- Distel, J. R., et al. (1999), The Combined X-ray Dosimeter (CXD) on GPS Block IIR Satellites, *Tech. Rep. LA-UR-99-2280*, Los Alamos Natl. Lab., Los Alamos, N. M.
- El-Aloui, M., M. Ashour-Abdalla, R. L. Richard, M. L. Goldstein, J. M. Weygand, and R. J. Walker (2010), Global magnetohydrodynamic simulation of reconnection and turbulence in the plasma sheet, *J. Geophys. Res.*, **115**, A12236, doi:10.1029/2010JA015653.
- Erickson, G. M., and R. A. Wolf (1980), Is steady state convection possible in the Earth's magnetotail, *Geophys. Res. Lett.*, **7**, 897, doi:10.1029/GL07i011p00897.
- Escobedo, M., S. Mischler, and M. A. Valle (2003), Homogeneous Boltzmann equation in quantum relativistic kinetic theory, *Electron. J. Differ. Equations*, **4**, 1.
- Eyni, M., and R. Steinitz (1978), Cooling of slow solar wind protons from the Helios 1 experiment, *J. Geophys. Res.*, **83**, 4387, doi:10.1029/JA083iA09p04387.
- Farrugia, C. J., V. A. Osherovich, and J. Fainberg (1999), Tensor nature of the gas pressure and measurements of the polytrophic indices for magnetic clouds: A case study, *AIP Conf. Proc.*, **471**, 499, doi:10.1063/1.58683.
- Fitts, D. D., and J. F. Mucci (1962), The Boltzmann H-function, *J. Chem. Educ.*, **39**, 515, doi:10.1021/ed039p515.
- Fok, M.-C., T. E. Moore, and W. N. Spjeldvik (2001), Rapid enhancement of radiation belt electron fluxes due to substorm dipolarization of the geomagnetic field, *J. Geophys. Res.*, **106**, 3873, doi:10.1029/2000JA000150.
- Freeman, J. W. (1988), Estimates of solar wind heating inside 0.3 AU, *Geophys. Res. Lett.*, **15**, 88, doi:10.1029/GL015i001p00088.
- Freeman, J. W., and R. E. Lopez (1985), The cold solar wind, *J. Geophys. Res.*, **90**, 9885, doi:10.1029/JA090iA10p09885.

- Fritz, T. A., and J. Chen (1999), The cusp as a source of magnetospheric particles, *Radiat. Meas.*, **30**, 599, doi:10.1016/S1350-4487(99)00239-5.
- Fritz, T. A., J. Chen, and R. B. Sheldon (2000), The role of the cusp as a source for magnetospheric particles: A new paradigm?, *Adv. Space Res.*, **25**(7–8), 1445, doi:10.1016/S0027-1177(99)00656-0.
- Fritz, T. A., M. Alothman, J. Bhattacharjya, D. L. Matthews, and J. Chen (2003), Butterfly pitch-angle distributions observed by ISEE-1, *Planet. Space Sci.*, **51**, 205, doi:10.1016/S0032-0633(02)00202-7.
- Fujimoto, M., T. Mukai, A. Matsuoka, Y. Saito, H. Hayakawa, S. Kokubun, and R. P. Lepping (2000), Multi-point observations of cold-dense plasma sheet and its relation with tail-LLBL, *Adv. Space Res.*, **25**, 1607, doi:10.1016/S0027-1177(99)00674-2.
- Goertz, C. K. (1978), Energization of charged particles in Jupiter's outer magnetosphere, *J. Geophys. Res.*, **83**, 3145, doi:10.1029/JA083iA07p03145.
- Goertz, C. K., and W. Baumjohann (1991), On the thermodynamics of the plasma sheet, *J. Geophys. Res.*, **96**, 20,991, doi:10.1029/91JA02128.
- Goertz, C. K., R. A. Smith, and L.-H. Shan (1991), Chaos in the plasma sheet, *Geophys. Res. Lett.*, **18**, 1639, doi:10.1029/91GL01782.
- Goldstein, B. E., M. Neugebauer, J. T. Gosling, S. J. Bame, J. L. Phillips, D. J. McComas, and A. Balogh (1995), Ulysses observations of solar wind plasma parameters in the ecliptic from 1.4 to 5.4 AU and out of the ecliptic, *Space Sci. Rev.*, **72**, 113, doi:10.1007/BF00768764.
- Gosling, J. (1999), On the determination of electron polytrope indices within coronal mass ejections in the solar wind, *J. Geophys. Res.*, **104**, 19,851, doi:10.1029/1999JA900254.
- Hilton, H. H. (1971), L parameter, a new approximation, *J. Geophys. Res.*, **76**, 6952, doi:10.1029/JA076i028p06952.
- Hones, E. W. (1963), Motions of charged particles trapped in the Earth's magnetosphere, *J. Geophys. Res.*, **68**, 1209, doi:10.1029/JZ068i005p01209.
- Hones, E. W., S. Singer, and C. S. R. Rao (1968), Simultaneous observations of electrons ($E > 45$ keV) at 2000-kilometer altitude and at 100,000 kilometers in the magnetotail, *J. Geophys. Res.*, **73**, 7339, doi:10.1029/JA073i023p07339.
- Horne, R. B., R. M. Thorne, S. A. Glauert, J. M. Albert, N. P. Meredith, and R. R. Anderson (2005), Timescale for radiation belt electron acceleration by whistler mode chorus waves, *J. Geophys. Res.*, **110**, A03225, doi:10.1029/2004JA010811.
- Horne, R. B., N. P. Meredith, S. A. Glauert, A. Varotsou, D. Boscher, R. M. Thorne, Y. Y. Shprits, and R. R. Anderson (2006), Mechanisms for the acceleration of radiation belt electrons, in *Recurrent Magnetic Storms*, *Geophys. Monogr. Ser.*, vol. 167, edited by B. T. Tsurutani et al., p. 151, AGU, Washington, D. C.
- Horne, R. B., R. M. Thorne, S. A. Glauert, N. P. Meredith, D. Pokhotelov, and O. Santolik (2007), Electron acceleration in the Van Allen radiation belts by fast magnetosonic waves, *Geophys. Res. Lett.*, **34**, L17107, doi:10.1029/2007GL030267.
- Huang, C. Y., C. K. Goertz, L. A. Frank, and G. Rostoker (1989), Observational determination of the adiabatic index in the quiet plasma sheet, *Geophys. Res. Lett.*, **16**, 563, doi:10.1029/GL016i006p00563.
- Huang, C. Y., L. A. Frank, G. Rostoker, J. Fennell, and D. G. Mitchell (1992), Nonadiabatic heating of the central plasma sheet at substorm onset, *J. Geophys. Res.*, **97**, 1481, doi:10.1029/91JA02517.
- Ingram, J. C., T. E. Cayton, R. D. Belian, R. A. Christensen, R. H. W. Friedel, M. M. Meier, G. D. Reeves, and M. Tuszeowski (2001), Substorm injection of relativistic electrons to geosynchronous orbit during the great magnetic storm of March 24, 1991, *J. Geophys. Res.*, **106**, 25,759, doi:10.1029/2000JA000458.
- Isenberg, P. A., C. W. Smith, W. H. Matthaeus, and J. D. Richardson (2010), Turbulent heating of the distant solar wind by interstellar pickup protons in a decelerating flow, *Astrophys. J.*, **719**, 716, doi:10.1088/0004-637X/719/1/716.
- Jeans, J. H. (1954), *The Dynamical Theory of Gases*, 4th ed., Dover, New York.
- Johnson, J. R., and S. Wing (2009), Northward IMF plasma sheet entropies, *J. Geophys. Res.*, **114**, A00D08, doi:10.1029/2008JA014017.
- Kaniadakis, G. (2009), Relativistic entropy and related Boltzmann kinetics, *Eur. Phys. J. A*, **40**, 275, doi:10.1140/epja/i2009-10793-6.
- Kaye, S. M., C. S. Lin, G. K. Parks, and J. R. Winckler (1978), Adiabatic modulation of equatorial pitch angle anisotropy, *J. Geophys. Res.*, **83**, 2675, doi:10.1029/JA083iA06p02675.
- Kozelova, T. V., B. V. Kozelov, and L. L. Lazutin (2000), Substorm large impulsive electric fields observed by CRRES, *Eur. Space Agency Spec. Publ.*, **SP-433**, 393.
- Kremser, G., A. Korth, S. L. Ullaland, S. Perraut, A. Roux, A. Pedersen, R. Schmidt, and P. Tanskainen (1988), Field-aligned beams of energetic electrons ($16 \text{ keV} \leq E \leq 80 \text{ keV}$) observed at geosynchronous orbit at substorm onsets, *J. Geophys. Res.*, **93**, 14,453, doi:10.1029/JA093iA12p14453.
- Kulcsrud, R. M. (1983), MHD description of plasmas, in *Handbook of Plasma Physics*, vol. 1, *Basic Plasma Physics I*, edited by M. N. Rosenbluth and R. Z. Sagdeev, pp. 115–145, North Holland, Amsterdam.
- Lavraud, B., and J. E. Borovsky (2008), The altered solar wind - magnetosphere interaction at low Mach numbers: Coronal mass ejections, *J. Geophys. Res.*, **113**, A00B08, doi:10.1029/2008JA013192.
- Lavraud, B., et al. (2009), Tracing solar wind plasma entry into the magnetosphere using ion-to-electron temperature ratio, *Geophys. Res. Lett.*, **36**, L18109, doi:10.1029/2009GL039442.
- Lazarus, A., J. Dasper, A. Szabo, and K. Ogilvie (2003), Solar wind streams and their interactions, *AIP Conf. Proc.*, **679**, 187, doi:10.1063/1.1618573.
- Lezniak, T. W., R. L. Arnoldy, G. K. Parks, and J. R. Winkler (1968), Measurements and intensity of energetic electrons at the equator at 6.6 RE, *Radio Sci.*, **3**, 710.
- Li, X., D. N. Baker, M. Temerin, T. E. Cayton, E. G. D. Reeves, R. A. Christensen, J. B. Blake, M. D. Looper, R. Nakamura, and S. G. Kanekal (1997), Multispacecraft observations of the outer zone electron variation during the November 3–4, 1993, magnetic storm, *J. Geophys. Res.*, **102**, 14,123, doi:10.1029/97JA01101.
- Lopez, R. E., H. Luhr, B. J. Anderson, P. T. Newell, and R. W. McEntire (1990), Multipoint observations of a small substorm, *J. Geophys. Res.*, **95**, 18,897, doi:10.1029/JA095iA11p18897.
- Lopez, R. E., H. E. H. Koskinen, T. I. Pulkkinen, T. Bosinger, R. W. McEntire, and T. A. Potemra (1993), Simultaneous observation of the poleward expansion of substorm electrojet activity and the tailward expansion of current sheet disruption in the near-earth magnetotail, *J. Geophys. Res.*, **98**, 9285, doi:10.1029/92JA02401.
- Lui, A. T. Y., R. E. Lopez, B. J. Anderson, K. Takahashi, L. J. Zanetti, R. W. McEntire, T. A. Potemra, D. M. Klumpar, E. M. Greene, and R. J. Strangeway (1992), Current disruption in the near-Earth neutral sheet, *J. Geophys. Res.*, **97**, 1461, doi:10.1029/91JA02401.
- Marino, R., L. Sorriso-Valvo, V. Carbone, A. Noullez, R. Bruno, and B. Bavassano (2008), Heating the solar wind by a magnetohydrodynamic turbulence energy cascade, *Astrophys. J.*, **677**, L71, doi:10.1086/587957.
- Marsch, E., W. G. Pilipp, K. M. Theime, and H. Rosenbauer (1989), Cooling of solar wind electrons inside 0.3 AU, *J. Geophys. Res.*, **94**, 6893, doi:10.1029/JA094iA06p06893.
- McDiarmid, I. B., and J. R. Burrows (1965), On an electron source fore the outer Van Allen radiation zone, *Can. J. Phys.*, **43**, 1161, doi:10.1139/p65-113.
- McIlwain, C. E. (1961), Coordinates for mapping the distribution of magnetically trapped particles, *J. Geophys. Res.*, **66**, 3681, doi:10.1029/JZ066i01p03681.
- Montgomery, D. C. (1971), *Theory of the Unmagnetized Plasma*, Gordon and Breach, New York.
- Neugebauer, M., P. C. Liewer, B. E. Goldstein, X. Zhou, and J. T. Steinberg (2004), Solar wind stream interaction regions without sector boundaries, *J. Geophys. Res.*, **109**, A10102, doi:10.1029/2004JA010456.
- Northrop, T. G., and E. Teller (1960), Stability of the adiabatic motion of charged particles in the Earth's field, *Phys. Rev.*, **117**, 215, doi:10.1103/PhysRev.117.215.
- Obara, T., Y. Miyoshi, and A. Morioka (2001), Large enhancement of the outer belt electrons during magnetic storms, *Earth Planets Space*, **53**, 1163.
- Ohtani, S., K. Takahashi, L. J. Zanetti, T. A. Potemra, R. W. McEntire, and T. Iijima (1991), Tail current disruptions in the geosynchronous region, in *Magnetospheric Substorms*, *Geophys. Monogr. Ser.*, vol. 64, edited by J. R. Kan et al., p. 131, AGU, Washington, D. C.
- Osherovich, V. A., V. A. Fainberg, R. G. Stone, R. J. MacDowall, and D. Berdichevsky (1997), Self-similar evolution of interplanetary magnetic clouds and Ulysses measurements of the polytropic index inside the cloud, *Eur. Space Agency Spec. Publ.*, **415**, 171.
- Osherovich, V. A., J. Fainberg, R. G. Stone, A. Vinas, R. Fitzenreiter, and C. J. Farrugia (1999), MHD of gas with polytropic index below unity and classification of magnetic clouds, *AIP Conf. Proc.*, **471**, 717, doi:10.1063/1.58718.
- Pagel, A. C., N. U. Crooker, T. H. Zurbuchen, and J. T. Gosling (2004), Correlation of solar wind entropy and oxygen ion charge state ratio, *J. Geophys. Res.*, **109**, A01113, doi:10.1029/2003JA010010.
- Paularena, K. I., J. D. Richardson, M. A. Olafsson, C. R. Jackson, and G. L. Siscoe (2001), A dawn-dusk density asymmetry in Earth's magnetosheath, *J. Geophys. Res.*, **106**, 25,377, doi:10.1029/2000JA000177.
- Pedersen, A. (1992), Substorm electric and magnetic field signatures on GEOS-1, GEOS-2, and ISEE-1, *Eur. Space Agency Spec. Publ.*, **ESA SP-335**, 237 pp.
- Pedersen, A., and C. P. Escoubet (1994), Substorm electric field measurements—Interpretations and lack of interpretations, paper presented at Second International Conference on Substorms, Univ. of Alaska Fairbanks, Fairbanks.

- Peredo, M., D. P. Stern, and N. A. Tsyganenko (1993), Are existing magnetospheric models excessively stretched?, *J. Geophys. Res.*, **98**, 15,343, doi:10.1029/93JA01150.
- Pfizer, K. A., T. W. Lezniak, and J. R. Winckler (1969), Experimental verification of drift-shell splitting in the distorted magnetosphere, *J. Geophys. Res.*, **74**, 4687, doi:10.1029/JA074i019p04687.
- Phan, T. D., and G. Paschmann (1996), Low-latitude dayside magnetopause and boundary layer for high magnetic shear: 1. Structure and motion, *J. Geophys. Res.*, **101**, 7801, doi:10.1029/95JA03752.
- Pierrard, V., and J. Lemaire (1996), Fitting the AE-8 energy spectra with two Maxwellian functions, *Radiat. Meas.*, **26**, 333–337, doi:10.1016/1350-4487(96)00057-1.
- Pudovkin, M. I. (1991), Physics of magnetospheric substorms: A review, in *Magnetospheric Substorms*, *Geophys. Monogr. Ser.*, vol. 64, edited by J. R. Kan et al., p. 17, AGU, Washington, D. C.
- Rastinkangas, R., V. Sergeev, G. Kremser, T. Ulich, H. Singer, and A. Korth (1994), Current disruption signatures at substorm onset observed by CRRES, paper presented at Second International Conference on Substorms, Univ. of Alaska Fairbanks, Fairbanks.
- Retzler, J., and J. A. Simpson (1969), Relativistic electrons confined within the neutral sheet of the geomagnetic tail, *J. Geophys. Res.*, **74**, 2149, doi:10.1029/JA074i009p02149.
- Roux, A., S. Perraut, A. Morane, P. Robert, A. Korth, G. Kremser, A. Pederson, R. Pellinen, and Z. Y. Pu (1991), Role of the near-Earth plasmashell at substorms, in *Magnetospheric Substorms*, *Geophys. Monogr. Ser.*, vol. 64, edited by J. R. Kan et al., p. 201, AGU, Washington, D. C.
- Sarris, E. T., S. M. Krimigis, and T. P. Armstrong (1976), Observations of magnetospheric bursts of high-energy protons and electrons at ~ 35 RE with Imp 7, *J. Geophys. Res.*, **81**, 2341, doi:10.1029/JA081i013p02341.
- Sarris, T., X. Li, and M. Temerin (2006), Simulating radial diffusion of energetic (MeV) electrons through a model of fluctuating electric and magnetic fields, *Ann. Geophys.*, **24**, 2583, doi:10.5194/angeo-24-2583-2006.
- Schindler, K. (1975), Plasma and fields in the magnetospheric tail, *Space Sci. Rev.*, **17**, 589, doi:10.1007/BF00718586.
- Schindler, K., and J. Birn (1978), Magnetospheric physics, *Phys. Rep.*, **47**, 109, doi:10.1016/0370-1573(78)90016-9.
- Schindler, K., and J. Birn (1982), Self-consistent theory of time dependent convection in the Earth's magnetotail, *J. Geophys. Res.*, **87**, 2263, doi:10.1029/JA087iA04p02263.
- Schulz, M., and A. Eviatar (1969), Diffusion of equatorial particles in the outer radiation zone, *J. Geophys. Res.*, **74**, 2182, doi:10.1029/JA074i009p02182.
- Schwartz, S. J., and E. Marsch (1983), The radial evolution of a single solar wind plasma parcel, *J. Geophys. Res.*, **88**, 9919, doi:10.1029/JA088iA12p09919.
- Selesnick, R. S., and J. B. Blake (2002), Relativistic electron drift shell splitting, *J. Geophys. Res.*, **107**(A9), 1265, doi:10.1029/2001JA009179.
- Skoug, R. M., W. C. Feldman, J. T. Gosling, D. J. McComas, and C. W. Smith (2000), Solar wind electron characteristics inside and outside coronal mass ejections, *J. Geophys. Res.*, **105**, 23,069, doi:10.1029/2000JA000017.
- Smith, C. W., W. H. Matthaeus, G. P. Zank, N. F. Ness, S. Oughton, and J. D. Richardson (2001), Heating of the low-latitude solar wind by dissipation of turbulent magnetic fluctuations, *J. Geophys. Res.*, **106**, 8253, doi:10.1029/2000JA000366.
- Sojka, J. J., and G. L. Wrenn (1985), Refilling of geosynchronous flux tubes as observed at the equator by GEOS 2, *J. Geophys. Res.*, **90**, 6379, doi:10.1029/JA090iA07p06379.
- Spence, H. E., and M. G. Kivelson (1990), The variation of the plasma sheet polytropic index along the midnight meridian in a finite width magnetotail, *Geophys. Res. Lett.*, **17**, 591, doi:10.1029/GL017i005p00591.
- Stawarz, J. E., C. W. Smith, B. J. Vasquez, M. A. Forman, and B. T. MacBride (2009), The turbulent cascade and proton heating in the solar wind at 1 AU, *Astrophys. J.*, **697**, 1119, doi:10.1088/0004-637X/697/2/1119.
- Stepanova, M., E. E. Antonova, D. Paredes-Davis, I. L. Ovchinnikov, and Y. I. Yermolaev (2009), Spatial variation of eddy-diffusion coefficients in the turbulent plasma sheet during substorms, *Ann. Geophys.*, **27**, 1407, doi:10.5194/angeo-27-1407-2009.
- Stepanova, M., T. Vucina-Parga, E. Antonova, I. Ovchinnikov, and Y. Yermolaev (2005), Variation of the plasma turbulence in the central plasma sheet during substorm phases observed by the interball/tail satellite, *J. Atmos. Sol. Terr. Phys.*, **67**, 1815, doi:10.1016/j.jastp.2005.01.013.
- Summers, D., and C. Y. Ma (2000), A model for generating relativistic electrons in the Earth's inner magnetosphere based on gyroresonant wave-particle interactions, *J. Geophys. Res.*, **105**, 2625, doi:10.1029/1999JA900444.
- Takahashi, K., L. J. Zanetti, R. E. Lopez, R. W. McEntire, T. A. Potemra, and K. Yumoto (1987), Disruption of the magnetotail current sheet observed by AMPTE/CCE, *Geophys. Res. Lett.*, **14**, 1019, doi:10.1029/GL014i010p01019.
- Thomsen, M. F., J. E. Borovsky, R. M. Skoug, and C. W. Smith (2003), Delivery of cold, dense plasma sheet material into the near-Earth region, *J. Geophys. Res.*, **108**(A4), 1151, doi:10.1029/2002JA009544.
- Tsyganenko, N. A. (1989), A magnetospheric magnetic field model with a warped tail current sheet, *Planet. Space Sci.*, **37**, 5, doi:10.1016/0032-0633(89)90066-4.
- Tuszewski, M. G., T. E. Cayton, and J. C. Ingraham (2002), A new numerical technique to design satellite energetic electron detectors, *Nucl. Instrum. Methods Phys. Res., Sect. A*, **482**, 653, doi:10.1016/S0168-9002(01)01735-1.
- Varotsou, A., D. Balcher, S. Bourdarie, R. B. Horne, S. A. Glauert, and N. P. Meredith (2005), Simulation of the outer radiation belt electrons near geosynchronous orbit including both radial diffusion and resonant interaction with whistler-mode chorus waves, *Geophys. Res. Lett.*, **32**, L19106, doi:10.1029/2005GL023282.
- Vörös, Z., et al. (2004), Magnetic turbulence in the plasma sheet, *J. Geophys. Res.*, **109**, A11215, doi:10.1029/2004JA010404.
- Walt, M. (1971), The radial diffusion of trapped particles induced by fluctuating magnetospheric fields, *Space Sci. Rev.*, **12**, 446, doi:10.1007/BF00171975.
- Wei-Ke, A., Q. Xi-Jun, S. Chun-Hua, and Z. Zhi-Yuan (2005), Dependence of the average Lorentz factor on temperature in relativistic plasmas, *Chin. Phys. Lett.*, **22**, 1176, doi:10.1088/0256-307X/22/5/042.
- Weygand, J. M., et al. (2005), Plasma sheet turbulence observed by Cluster II, *J. Geophys. Res.*, **110**, A01205, doi:10.1029/2004JA010581.
- Whang, Y. C., K. W. Behannon, L. F. Burlaga, and S. Zhang (1989), Thermodynamic properties of the heliospheric plasma, *J. Geophys. Res.*, **94**, 2345, doi:10.1029/JA094iA03p02345.
- Wienke, B. R. (1975), Mean, mean-square, and most-probable momentum for a relativistic Maxwellian ensemble, *Am. J. Phys.*, **43**, 317, doi:10.1119/1.10079.
- Williams, D. J., D. G. Mitchell, C. Y. Huang, L. A. Frank, and C. T. Russell (1990), Particle acceleration during substorm growth and onset, *Geophys. Res. Lett.*, **17**, 587, doi:10.1029/GL017i005p00587.
- Wing, S., and J. R. Johnson (2009), Substorm entropies, *J. Geophys. Res.*, **114**, A00D07, doi:10.1029/2008JA013989.
- Wing, S., and P. T. Newell (1998), Central plasma sheet ion properties as inferred from ionospheric observations, *J. Geophys. Res.*, **103**, 6785, doi:10.1029/97JA02994.
- Wing, S., J. W. Gjerloev, J. R. Johnson, and R. A. Hoffman (2007), Substorm plasma sheet ion pressure profiles, *Geophys. Res. Lett.*, **34**, L16110, doi:10.1029/2007GL030453.
- Zhu, X. M. (1990), Plasma sheet polytropic index as inferred from the FPE measurements, *Geophys. Res. Lett.*, **17**, 2321, doi:10.1029/GL017i013p02321.

J. E. Borovsky and T. E. Cayton, Los Alamos National Laboratory, Los Alamos, NM 87545, USA. (jborovsky@lanl.gov)